Article

Performance Assessment of Silica Gel-Water Solar Adsorption Refrigeration System in Egypt

Gamal B. Abdelaziz1, Hamdy H. El-Ghetany2, Mohamed A. Omara1, Ragab G. Abdel hady3

1   Mechanical Department, Faculty of Technology and Education, Suez University, Egypt.
2   Solar Energy Dept., National Research Centre, Dokki, 12622, Giza, Egypt.
3   Technical Education Teacher, Ministry of Education, Giza, Egypt.

Abstract: This work concerns an analytical study of the performance evaluation of a silica gel-water solar adsorption chiller. The study was conducted on Simulink software of an adsorption system of one ton of refrigeration (TR) capacity (3.5kW). Several parameters are studied to find out the effect of ambient air temperature, collector inlet, and the collector area on the temperature of the collector outlet, bed outlet adsorbate, condenser output adsorbate, and the thermal power of collector, bed, evaporator, Specific Cooling Power (SCP) and Coefficient of Performance (COP) at different seasons of the year. It is found that the system performance increased with increasing the ambient temperature and the collector area, while the performance system decreased with decreasing the collector output temperature for the previously mentioned studied parameters. Results indicated that the highest COP is achieved at the air temperature, the collector output temperature, and the area collector were 0.68, 0.68, and 0.81, respectively. Also, it was found that the highest SCP at the air temperature of 30°C, the collector output temperature of 75 °C, and the collector area of 14 m2 were 345W/kg, 355W/kg, and 626W/kg, respectively.

Keywords: MATLAB, Performance Assessment, Simulink, Adsorption Chiller, Silica gel-water, Solar Cooling.

1. Introduction and Literature Review:

The performance of a combined silica gel/water adsorption chiller with a closed cooling tower was presented by Chen et al. [1-2]. They developed the model without vacuum valves and evaluated its performance experimentally. The effect of heat and mass recovery time and comparison with other adsorption coolants on chiller performance were performed. A 1-D transient model has been introduced and validated by experimental results. The governing equations for the adsorption cooler were solved by Rezk et al. [3-7] using MATLAB to determine the thermophysical properties of the working fluids. They used the simulation model to investigate the effect of the distance between the fins on the cooler's performance. A comparison was made between some adsorbents regarding water absorption, namely RD-2060, HKUST-1, Fe-BTC, and silica gel. The results showed that the HKUST-1 adsorbent had a better water absorption rate of 96 % than silica gel.

Wang et al. [8] The adsorption deterioration of silica gel in the silica gel–water adsorption refrigeration system was theoretically and experimentally verified. The results indicated that many factors influenced the adsorption capacity of the silica gel. The major cause of the decrease in adsorption capacity was contamination by solid particles. The performance of solar-powered adsorption cooling systems working under the climate conditions of the Middle East region has been theoretically investigated by El-sharkawy et al. [9]. The results were investigated using actual Cairo/Aswan solar measurements in Egypt and the coastal city of Jeddah in Saudi Arabia. Two system arrangements have been proposed: without hot water buffer storage and with hot water buffer storage. The findings indicate that

the overall cyclic cooling Power of the system operating under the climatic conditions of Cairo and Jeddah is approximately 14.8 kW and 15.8 kW for the climatic conditions of Aswan. Theoretical results showed that the hot water buffer storage system has a higher average daily cooling capacity and average daily COP.

For drinking water production, the impact of condenser and evaporator temperatures on adsorption efficiency was studied by Youssef et al. [10]. Results showed that more water was released as the condenser temperature decreased, and a higher specific cooling capability was achieved. In addition, similar changes in water production and cooling have been made as the temperature of the evaporator rises. A silica gel/water absorption modulated refrigeration unit was experimentally investigated by Khalil et al. [11]. The effects of evaporator pressure, evaporator inlet water temperature, initial silica gel temperature, hot air regeneration temperature, and mass flow rate on the chiller's performance were investigated. The results showed that the increases in the hot air regeneration temperature and the inlet evaporator temperature increased the unit cooling capacity and COP. In contrast, lower silica gel temperatures and evaporator pressures improved unit cooling capacity and COP. The adsorption refrigeration system using silica gel/water was experimentally studied by Kumar et al. [12]. The system has been evaluated for various operating temperatures and refrigeration effects versus cycle time. They showed that a regeneration temperature from 60 °C to 80 °C is sufficient to carry out the desorption cycle and produce cooling at the evaporator. Also, it was seen that the adsorption is more at the beginning of the cycle and decreases with an increase in cycle time due to the saturation of the adsorbent.

A simulation model for evaluating the silica gel/water adsorption system performance was developed by Najeh et al. [13-16]. The model examined the effect of physical factors like temperature and pressure in the system components to adjust and maximize efficiency during cold output. The experimental observations agree well with the mathematical model results.

Szelgowski and Grzebielec [17] compared the performance of silica gel/water and activated carbon/methanol adsorption chillers. A special control algorithm device has been developed and implemented to perform the correct action, which allows for keeping the temperature in the evaporator at a preset level. An energy efficiency rating (EER) was obtained at level 0.14 for activated carbon methanol and level 0.25 for the silica gel water working pair. The Specific Cooling Power was 208 W/kg for silica gel water and 16 W/kg for activated carbon methanol.

Lim et al. [18] experimentally analyzed the adsorption process in a closed thermal energy storage system under non-isothermal and non-isobaric conditions with silica gel/water. Experiments were conducted to investigate the impact of the temperature change on the evaporator and the mass variation of the water in the evaporator. Through the test results, an increased evaporator temperature leads to an increased uptake amount because of the larger pressure difference and vapor mass flow rate. Also, a simple system's measured adsorption isotherm value was approximately 29.8–56.7 % of the theoretical estimation.

Mitra et al. [19, 20] An improved simulation study of an air-cooled, 2-stage, 2-bed silica gel/water adsorption system was carried out, investigated the system performance for the various heat sources of 65–85 °C and chilled water inlets of 11.5–24 °C, operating with an ambient temperature of 36 °C. The optimum half-cycle time for this system is found to increase from 30 min to 50 min when the heat source temperature decreases from 85 °C to 65 °C. In contrast, it is insensitive to chilled water temperature variation. The COP was observed to be relatively insensitive to such alterations.

Ntsoane et al. [21] studied the performance evaluation of a silica gel/water adsorption-based cooling system for mango fruit storage in Sub-Saharan Africa. The prototype of the cooling device based on adsorption was tested for its ability to store fresh mangoes, resulting in a mass loss of 3 % of fruits at an average air temperature of 15 °C and 90 % relative humidity. It was a cooling efficiency evaluation of the adsorption-based refrigerator cooling (prototype) at various cooling periods (30 to 120 minutes) with the renewal intervals set for 30 minutes and different degrees of hot water regeneration temperature (60, 70, and 80 °C). The findings revealed that the cooling cycle time has a more significant effect on the low storage temperature, while the original model's cooling potential is improved by increasing the hot water temperature and cooling cycle time.

The fin design parameter's effect on heat transfer inside the bed and system performance was studied analytically by Abd-Elhady and Hamed [22]. The influence of different factors on adsorption chiller performance and its performance coefficients was studied in this model (COP). Bed geometry parameters: fin spacing, radius, and thickness directly influenced chiller performance. Reducing the distance between fins increases heat transmission. The average cooling performance for optimal operating circumstances was up to 147.6%, with a reduction in fin spacing from 0.4 cm to 0.2 cm, while raising the fin radius reduced the adsorption temperature. The specific cooling ability

is increased by lowering the acceptable radius from 16 mm to 8 mm to an average value of 44%. The fine thickness affects the heat transmission in the bed just a little.

Kilic and Anjrini [23] created, examined and assessed two models that combined adsorption and compression cooling systems. The first model (Type A) linked the adsorption refrigeration system evaporator and the compression refrigeration system condenser. The second model (Type B) connected the serial evaporators by connecting the adsorption refrigeration and the compression refrigeration system evaporator. Three adsorbents were employed (RD silica gel, RD silica gel 2060, and silica gel-Li Cl When the effect of different ambient temperatures and cycle times for each of the two models was considered, the results showed that the temperature evaporator increased with the decrease in the performance coefficient in Type A and increased with the increase in the performance coefficient in Type B.

Elsheniti et al. [24] designed a laboratory model of a silica gel/water adsorption cooling system and evaluated its performance under different operating conditions. The experimental results showed an increase in the coefficient of performance and specific cooling capacity with the increase in the temperature of the hot and coolant water and a decrease in the cooling water temperature.

A solar adsorption refrigeration system simulation was performed by Mostafa et al. [25] under different atmospheric conditions, while Missaoui et al. [26] designed and evaluated the performance of different designs of solar adsorption cooling systems with and without heat storage. The designs were compared regarding solar collector area, heat storage tank size, and adsorption coolant cycle time. The results showed that the system improves when a stratified hot water tank is used instead of a thoroughly mixed hot water tank. It was discovered that the system using a hot water tank produces stable cooling Power and is better than the direct connection system. The cooling capacity increased with the increases of the adsorption cycle time, the solar collector's area, and the water tank's volume. Wang et al. [27] studied and analysed the variation of heat transfer properties of a silica gel/water adsorption-cooled system and compared a vacuum tube bed reinforced with and without fins. The performance coefficient analysis of the system showed that the more fins, the better. The experimental results also showed that the greater the number of fins, the greater the specific cooling capacity. El-Ghetany et al. [28] designed a silica gel/water adsorption refrigeration system using MATLAB program to design the system from 10 to 100 tons of cooling. Results indicated an increase of cooling load with the increase of the area of the condenser, evaporator, and other independent parameters.

This study aims to evaluate the performance of a silica gel/water solar adsorption cooling system with a capacity of 3.5 kW. The effect of the operating conditions on the system performance did not covered in the previous literature review. A theoretical study of the effect of ambient air temperature at some months of the year using MATLAB program will be performed. Performance values by the collector water outlet temperature, the collector efficiency, the collector thermal power, the bed thermal power, the collector water inlet temperature, the bed outlet adsorbate temperature, the condenser output adsorbate temperature, the thermal evaporator power, Coefficient of Performance (COP) and Specific Cooling Power (SCP).

2. Description of the System:

Figure 1 shows a silica gel water adsorption refrigeration system. The system contains three sections: The refrigeration unit contains a water-cooled evaporator, an air-cooled condenser, and an expansion device. The second section is a heat exchanger consisting of two beds with a coil of copper, and around them are silica gel and water. Finally, the third section is the source of heat: the solar collector. The adsorption cycle consists of four processes: preheating, adsorption, pre-cooling, and adsorption. The evaporator valve is closed during preheating, and hot water is circulated in a layer to increase the bed's pressure. When the bed pressure becomes higher than that in the condenser, it is connected to the condenser, and the absorption process begins. Water vapor separates from the silica gel due to further heating and moves to the condenser, where it condenses. After the adsorption, the bed valve is closed from the condenser, and the cooling water is circulated in the adsorption bed, called the pre-cooling process. Due to the passage of cooling water, the pressure in the bed decreases and becomes lower than in the evaporator. At this moment, the adsorbent bed is connected to the evaporator, and the evaporated water vapor exits the adsorption device and is adsorbed on the silica gel. During the adsorption process, cooling water is continuously supplied to the bed to eliminate the adsorption heat.
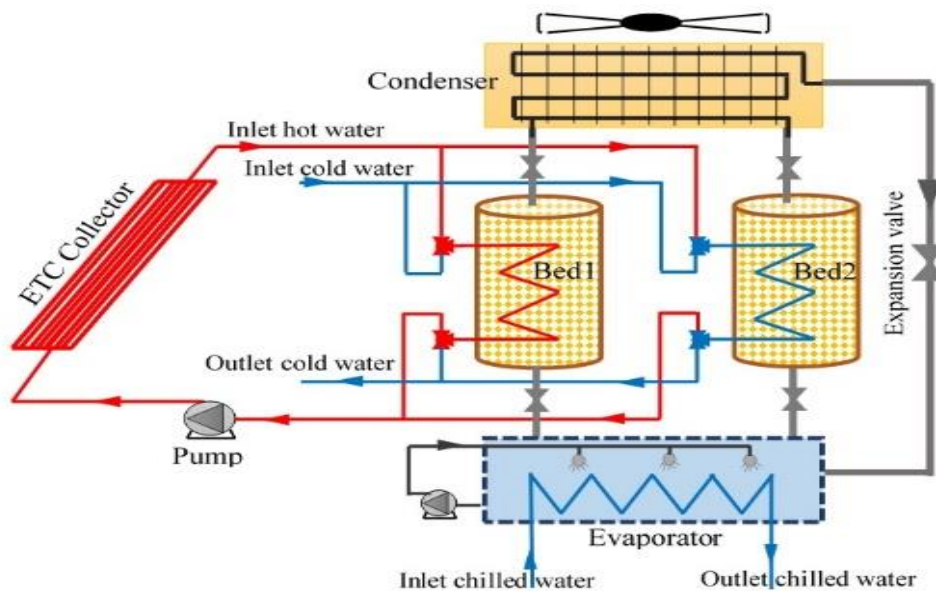
Fig.1 Schematic of two-bed adsorption chiller

3. Modeling for Adsorption Chiller:

Evaluating the performance of an adsorption refrigeration system requires iterative programming to calculate complex flows (recirculation and reverse flow). Simulink, created by MATLAB, was chosen because it is very flexible and can handle unstable situations. The model is built according to the performance calculation method. The user selects the operating conditions as shown in Table 1, and the program calculates the coefficient of performance, specific cooling Power, and others, as explained later.

Fig. 2 presents a Simulink schematic representation for the cooling system consisting of four main components describing the governing equations for the condenser, adsorber beds, solar collector, and evaporator.
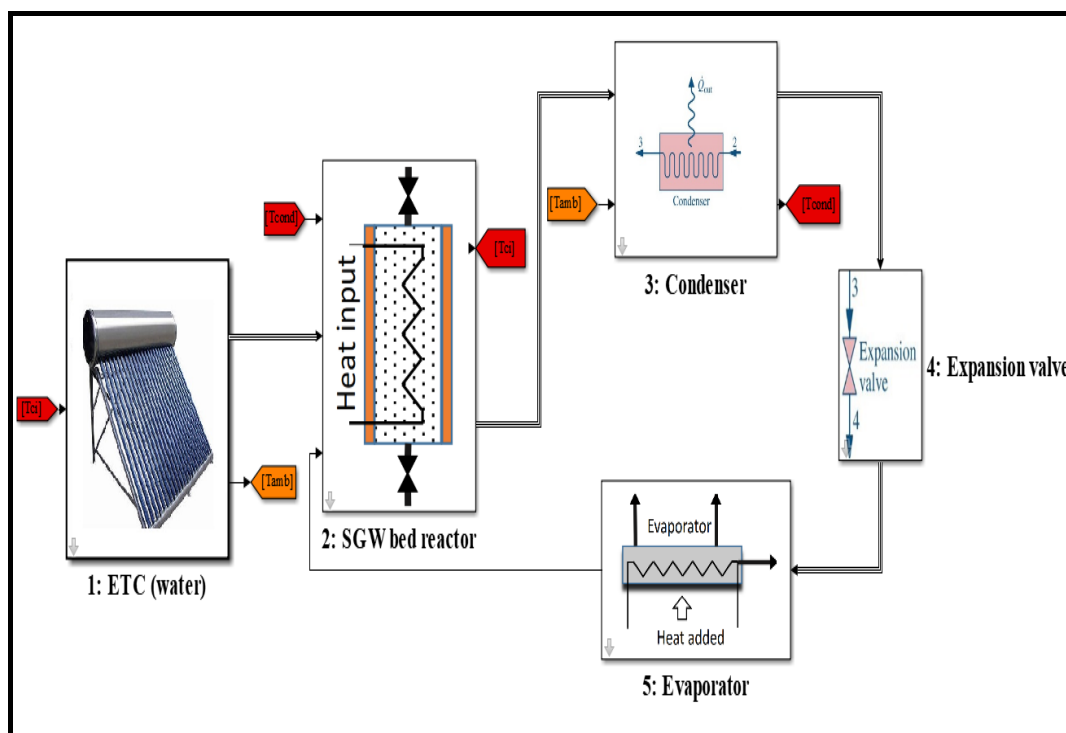

Fig. 2 schematic diagram of the Simulink model.

Table1. Operating conditions

The moist important data	Typical Values	
Temperature of evaporator	10	[°C]
Temperature of condenser	43	[°C]
Inlet chilled water temperature	25	[°C]
The mass flow rate of air	0.9	[kg/s]
Operating Hours	6	[hr]
Refrigerant flow rate	0.0015	[kg/s]
Chilled water flow rate	0.08	[kg/s]
Evaporator coil thermal conductivity	0.151	[W/m.K]
Mass of silica gel	22.8	[kg]
bed coil thermal conductivity	0.15	[W/m.K]
ETC area	14.65	[m2]
ETC mass flow rate	1.4	[kg/s]
Water/SG ratio, kg/kg	0.23	--
Cooling Load	1	TR

4. Mathematical Model

Figure 3 presents the simulation flow chart of the solar silica gel/water system. It was necessary to design an adsorption cooling system at different cooling loads before we evaluated its performance according to the factors affecting the system's performance.
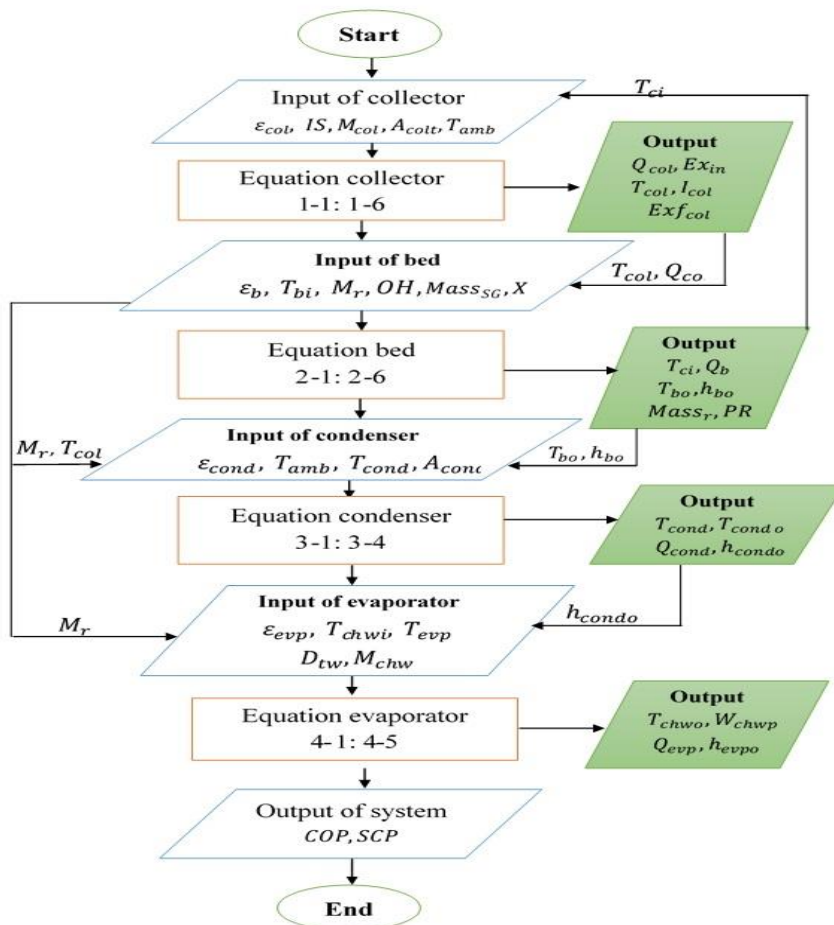

Fig. 3 Flow chart of the model

The best design for each cooling load was achieved as described in Ref. [28]. Therefore, a cooling system with a cooling capacity of 1 TR was chosen to evaluate its performance theoretically on the MATLAB program. Some variables extracted from the design model had to be entered when entering the program, as shown in Table 1. The energy balance for each part of the system was made within the program; its variables were adjusted, and its accuracy was tested

4.1 Mathematical model of solar collector

Figure 4 describes the solution procedure where the input parameters are simulated via the software program, and the solar collector simulation results are issued. The collector mathematical model can be presented below:

Thermal useful load, kW:

$$Q_{col} = Is \times A_{colt} \times \eta_{col} \qquad\qquad 1\text{-}1$$

Collector temperature difference, °C:

$$dT_{col} = \frac{Q_{col}}{CP_w \times M_{col}} \qquad\qquad 1\text{-}2$$

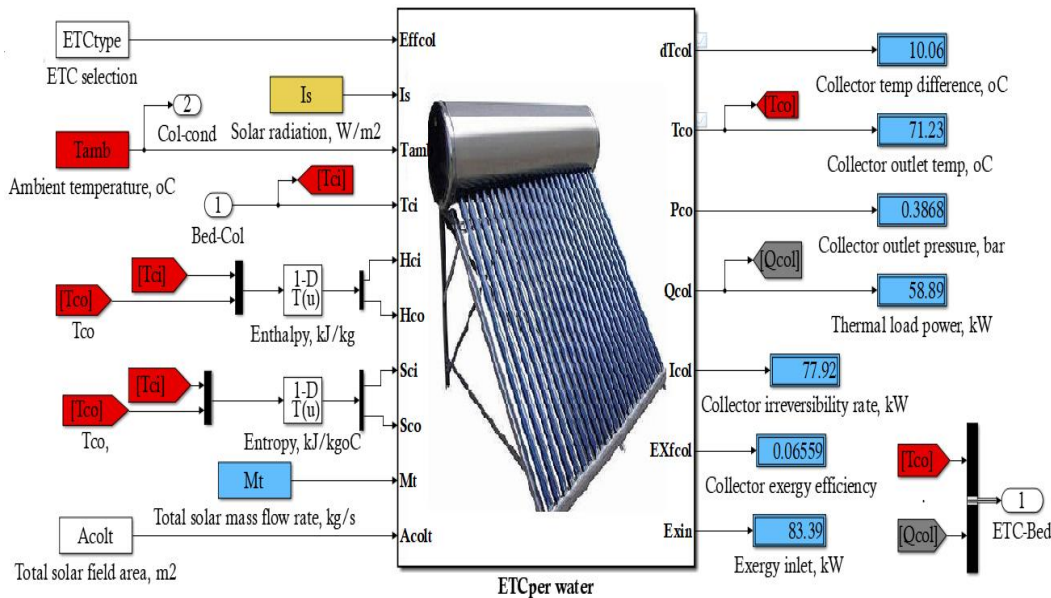$$T_{co} = T_{ci} + dT_{col} \qquad\qquad 1\text{-}3$$

Fig. 4 Simulink model of the solar collector

Collector irreversibility rate, kW

$$I_{col} = \left[\frac{A_{col} \times Is}{1000} \times \left(1 - \frac{T_{amb} + 273}{6000}\right)\right] + [M_{col} \times (h_{ci} - h_{co})] - [(T_{amb} + 273) \times (S_{ci} - S_{co})] \qquad 1\text{-}4$$

Exergy inlet, kW:

$$Ex_{in} = \frac{A_{col} \times Is}{1000} \times (1 - \frac{T_{amb} + 273}{6000}) \qquad\qquad 1\text{-}5$$

Exergy efficiency:

$$\eta_{Ex,col} = 1 - \frac{I_{col}}{Ex_{in}} \qquad\qquad 1\text{-}6$$

4,2 Mathematical model of the bed:

Figure 5 shows the Simulink model of the bed. The parameters are entered, the simulation procedure with the governing equations of the bed energy balance is issued, and the bed simulation outputs results.
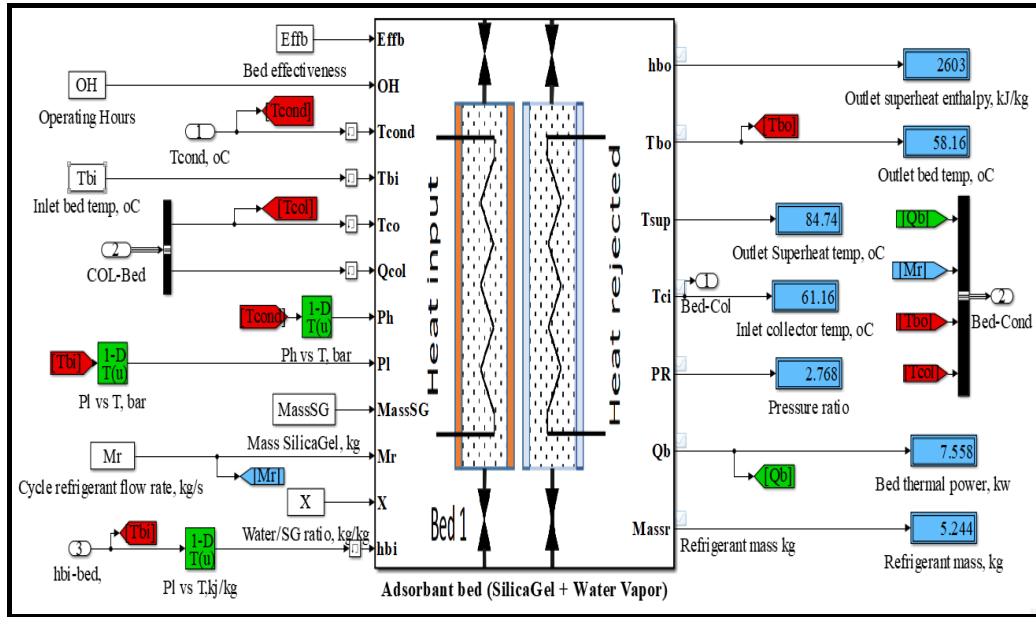
Fig. 5 Bed Simulink model

Bed thermal power, kW:

$$Q_{bed} = \frac{Q_{col} * \eta_b}{OH}$$ 2-1

The temperature of exit ref. Bed, oC:

$$T_{b,o} = \eta_b \times (T_{co} - T_{bi}) + T_{bi}$$ 2-2

Pressure Ratio

$$PR = \frac{P_{cond}}{P_{evp}}$$ 2-3

Outlet enthalpy:

$$h_{bo} = \left(\frac{Q_{bed}}{M_r}\right) + h_{bi}$$ 2-4

Inlet temperature, °C:

$$T_{c,i} = T_{co} - (\eta_b \times (T_{co} - T_{b,i}))$$ 2-5

Refrigerant mass, kg:

$$Mass_r = Mass_{SG} * X$$ 2-6

4,3 Mathematical model of the condenser:

Figure 6 shows an adsorption condenser simulation model. The parameters received from the bed are entered, and the simulation performs the energy conservation of the air-cooled condenser unit.

Condenser thermal power, kW:

$$Q_{cond} = M_r \times (h_{cond,i} - h_{cond,o})$$ 3-1

Condenser refrigerant out temperature, °C:

$$T_{cond,o} = T_{bo} - \left[\frac{(T_{cond} - T_{amb})}{\eta_{cond}}\right] \tag{3-2}$$

Condenser temperature °C:

$$T_{cond} = T_{amb} + \left[\frac{Q_{cond}}{(Cp_{air} \times M_{air})}\right] \tag{3-3}$$

Total heat loss, kW/m2 °C:

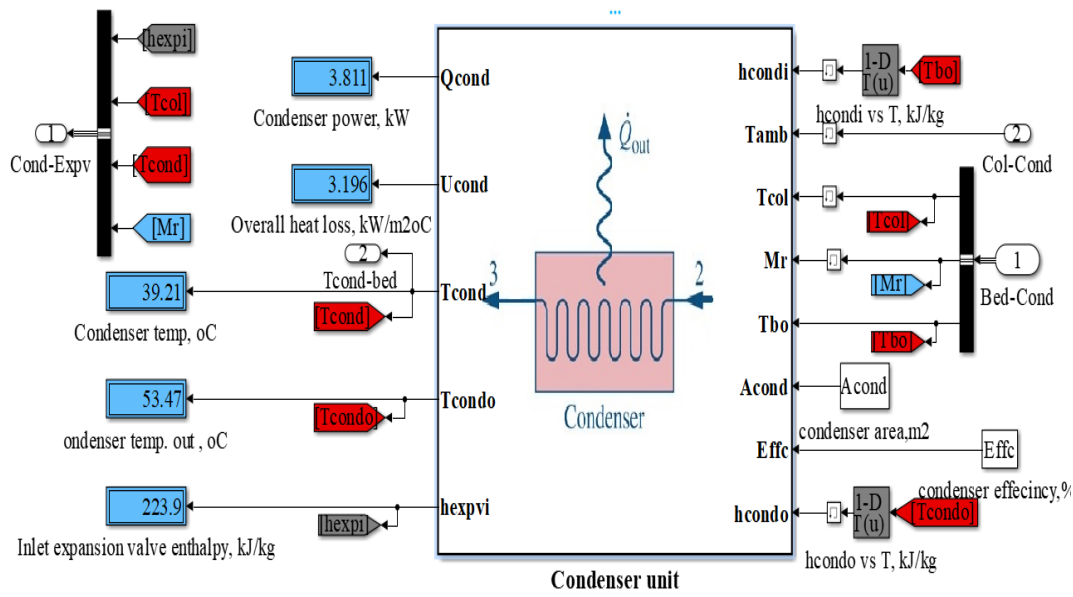$$U_c = \frac{Q_{cond}}{A_{cond} \times (T_{cond} - T_{amb})} \tag{3-4}$$

Fig. 6 Condenser unit Simulink model

4.4 Mathematical model of the evaporator:

Figure 7 shows a simulation of an evaporator. The parameters received from the condenser are entered, and the energy balance simulation of the water-cooled evaporator unit is performed. Then, the values are extracted and used to evaluate the system's performance.

Evaporator thermal power, kW:

$$Q_{evp} = M_{ch.w} \times Cp_w \times (T_{ch,w,i} - T_{ch,w,o}) \tag{4-1}$$

Outlet chilled water temperature, °C:

$$T_{ch,w,o} = T_{ch,w,i} - (\eta_{evp} * (T_{ch,w,i} - T_{evp})) \tag{4-2}$$

Outlet enthalpy of the evaporator, kJ/kg:

$$h_{evp,o} = \left(\frac{Q_{evp}}{M_r}\right) + h_{evp,i} \tag{4-3}$$

The velocity of water, m/s:

$$V_{ch,w} = \frac{M_{ch.w}}{\rho_w \times (\pi/4) \times D_{tw}^2} \tag{4-4}$$

Pump Power, kW:

$$W_{ch,w,p} = \rho_w \times (\pi/4) \times D_{tw}^2 \times V_{ch,w} \times Cp_w \times (T_{ch,w,i} - T_{ch,w,o}) \tag{4-5}$$
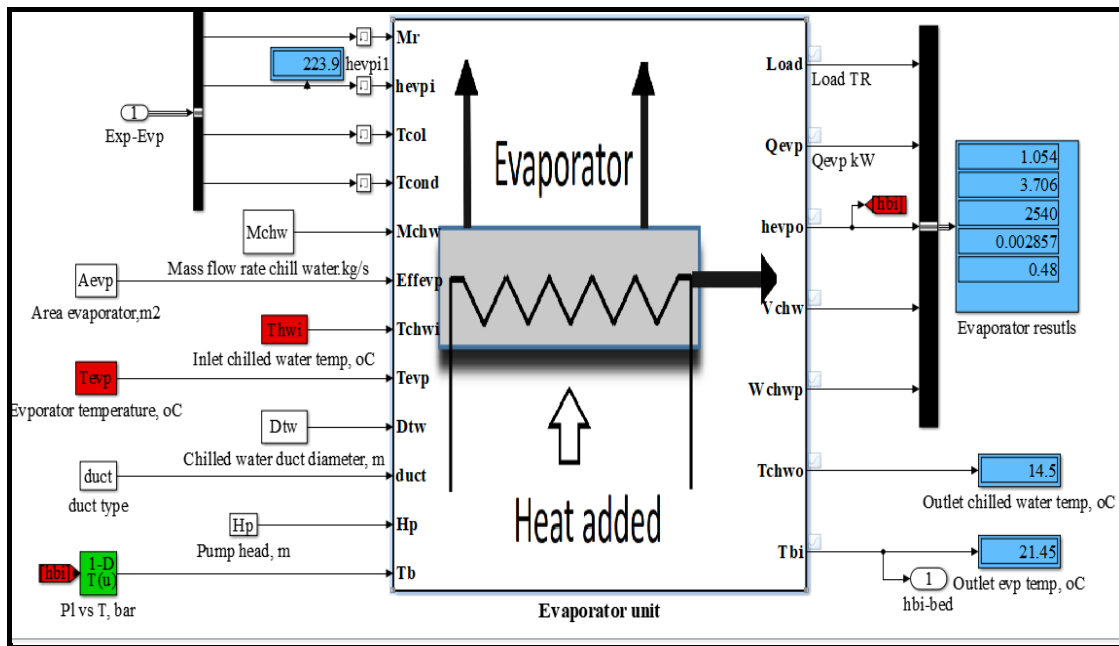
Fig. 7 Simulink model of the Evaporator

4,5: Performance of the System:

The system performance can be evaluated by the cycle coefficient of performance (COP):

$$COP_{system} = \frac{Q_{evp}}{Q_{bed}} \qquad\qquad 5\text{-}1$$

$$COP_{solar\ system} = \frac{Q_{evp}}{A_{co} \times IS} \qquad\qquad 5\text{-}2$$

The specific cooling power SCP (W/kg) is used when producing chilled water. The SCP is the ratio between the refrigeration capacity per unit mass of adsorbent:

$$SCP = \frac{Q_{evp}}{Mass_{SG}} \qquad\qquad 5\text{-}3$$

5. Results and Analysis:

The adsorption cooling system performance is characterized by many factors, such as the temperature and flow rate of hot water, the dimensions and materials of the bed, the ambient temperature, the solar collector area, solar radiation, and others. This research studies the effect of ambient temperature (15 °C to 45 °C), the collector water outlet temperature (60 °C to 90 °C), and the collector area (10 m2 to 20 m2) on system performance. Four months were analysed according to the year's seasons, namely January, April, July, and October, to evaluate the system's performance.

5.1 Effect of the ambient temperatures:

Figure 8 shows the ambient temperature's effect on the collector's water temperature outlet for different seasons. The figure indicates that the collector water outlet temperature increased with an increase in ambient temperature all year. In April, the collector water outlet temperature increased from 72 °C to 84 °C with an increase of 14.3 % when the ambient temperature changed from 15 °C to 45 °C. At the ambient temperature of 30 °C, the collector water outlet temperature increases with different seasons. It was also found that the highest collector water outlet temperature was in July, followed by April, October, and January. In interpreting the results, we find that the main reason the collector water outlet temperature increased was the solar radiation falling on it.
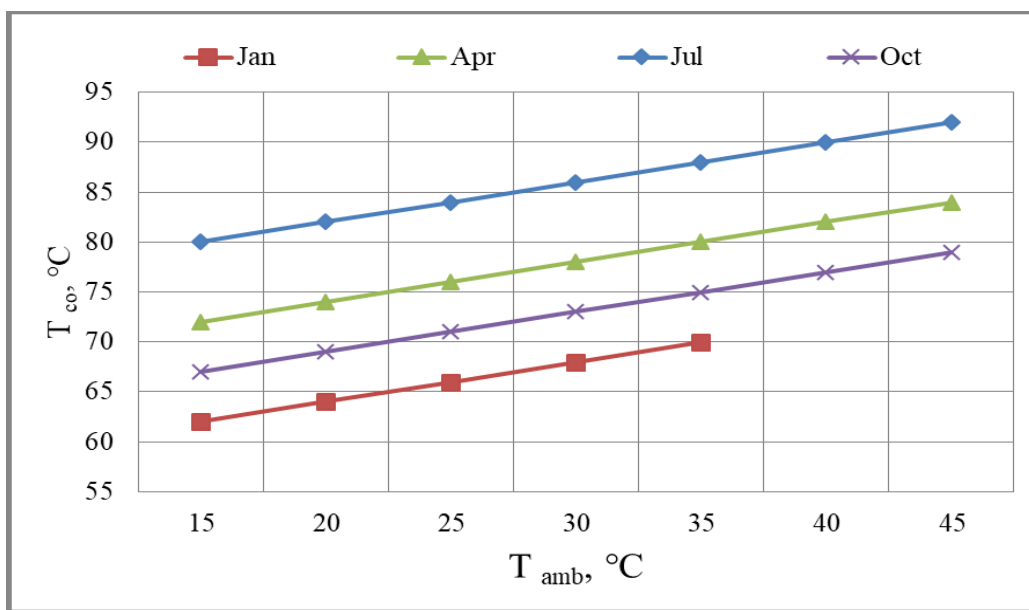
Fig. 8 Effect of ambient temperature on the water temperature outlet of the collector for different seasons

Figure 9 illustrates the ambient temperature's effect on the collector efficiency. It shows that the collector efficiency increased with an increase in ambient temperature all year. In April, the collector efficiency increased from 0.636 to 0.673, with an increase of 5.5 % when the atmospheric temperature changed from 15 °C to 45 °C. When the ambient temperature of 30 °C, the collector efficiency decreases with the months of the year. It was also found that the highest collector efficiency was in January, October, April, and July.
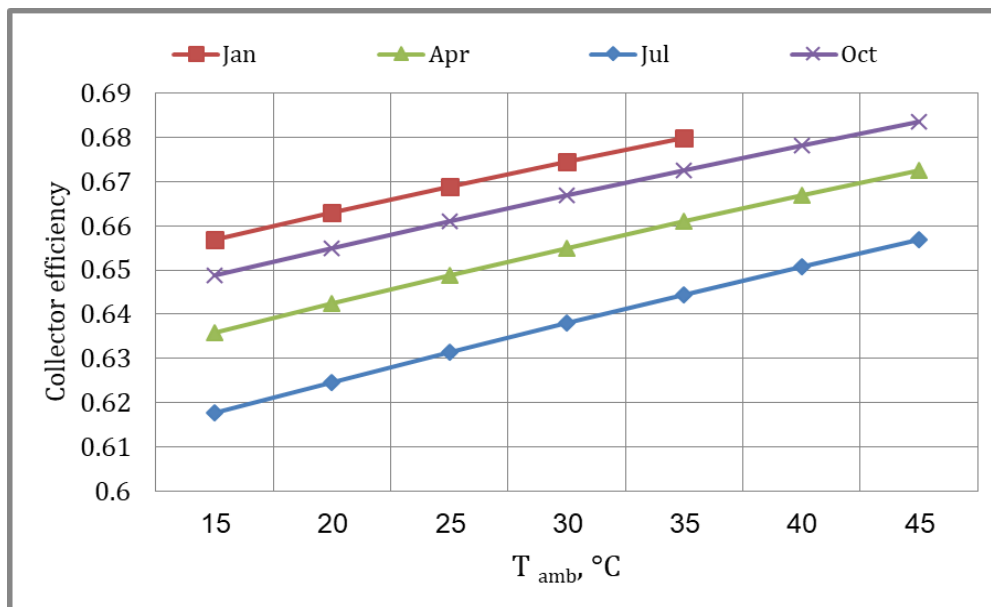

Fig. 9 Effect of ambient temperature on the collector efficiency for different seasons

Figure 10 shows the atmospheric temperature's effect on the thermal power of the collector for different seasons. It introduces an increased collector thermal power as the ambient temperature increases. In April, the thermal power collector increased from 57.77 kWh to 61.11 kWh, with an increase of 5.8 %, when the ambient temperature changed from 15 °C to 45 °C with an increase of 200 %. It is found that for the case of the ambient temperature of 30 °C, the thermal power of the collector increases with the months of the year. It was also found that the highest thermal power of the collector was in July, April, October, and January. The reason for increasing the thermal energy of the collector was the solar radiation and the collector's efficiency.
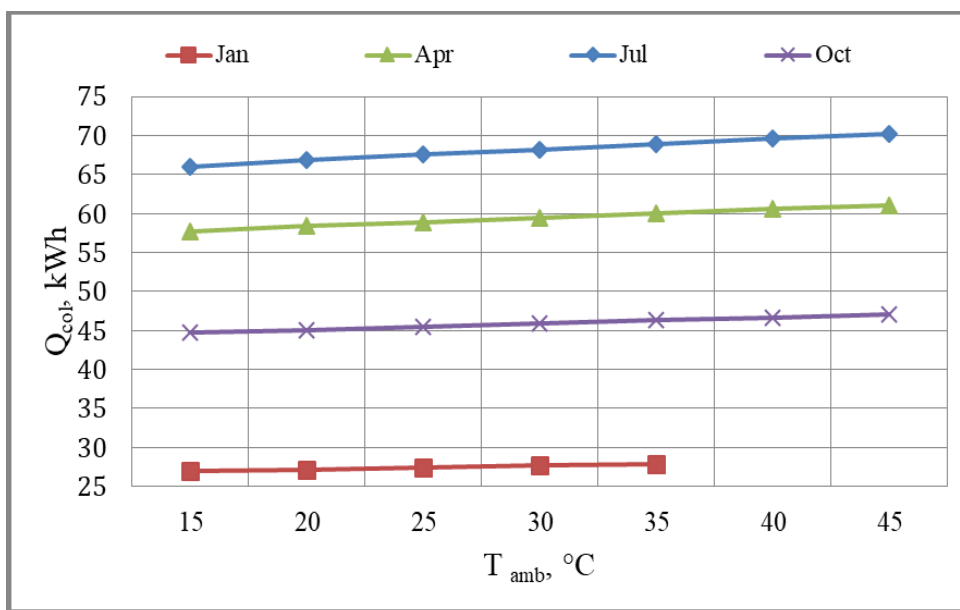
Fig. 10 Effect of ambient temperature on the thermal power of the collector for different seasons

Figure 11 shows the ambient temperature's effect on the thermal power of the bed for different seasons. The figure indicates that the thermal power of the bed increased when the ambient temperature increased. For example, in the case of April, the thermal power of the bed increased from 9.63 kW to 10.18 kW, with an increase of 5.7 %, when the ambient temperature changed from 15 °C to 45 °C with an increase of 200 %. It was also found that the highest thermal power of the bed was in July, April, October, and January. The increased thermal power of the bed is due to the increase in the temperature of the collector with constant adsorption time, which leads to faster evaporation of the water in the silica gel.
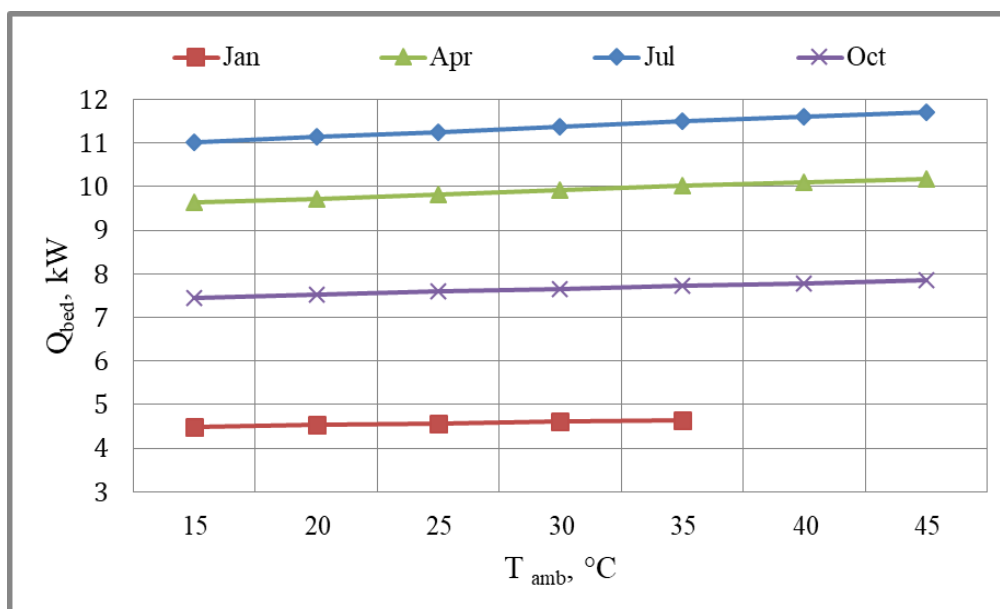

Fig. 11 Effect of ambient temperature on the bed's thermal power for different seasons

Figure 12 shows the ambient temperature's effect on the collector's water temperature inlet for different seasons. The figure indicates that the collector water inlet temperature increased when the ambient temperature increased. In April, the collector water inlet temperature rises from 62.13 °C to 73.56 °C with an increase of 18.4 % when the ambient temperature changes from 15 °C to 45 °C. The figure shows that at an ambient temperature of 30 °C, the collector water inlet temperature increases with all seasons. It was also found that the highest collector water outlet temperature was in July, followed by April, October, and January. As a result of the heat exchange inside the bed

between the adsorbate and the water collector led to an increase in the temperature difference of the collector water. The collector is affected by the ambient air temperature, which increases the collector's thermal power, leading to an increase in the collector water inlet temperature. The results showed that the increased solar radiation increased the collector water inlet temperature and the bed output adsorbate temperature.
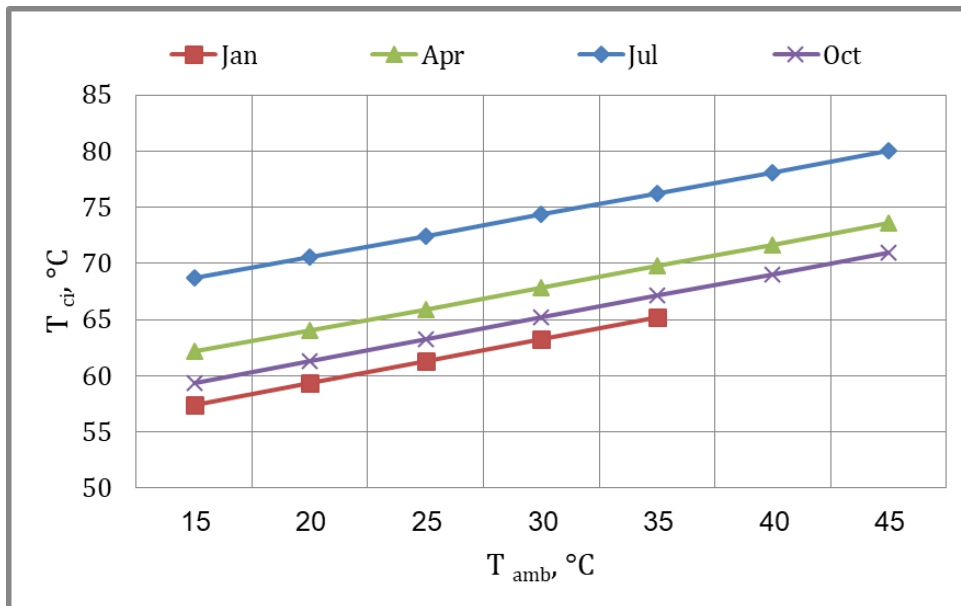

Fig. 12 Effect of ambient temperature on the collector water inlet temperature for different seasons

Figure 13 shows the effect of ambient temperature on the bed output adsorbate temperature for different seasons. The figure indicates that the bed output adsorbate temperature increased when the ambient temperature increased. In April, the bed outlet adsorbate temperature increased from 59.18 °C to 70.94 °C, an increase of 19.8 %, when the ambient temperature changed from 15 °C to 45 °C, an increase of 200 %.
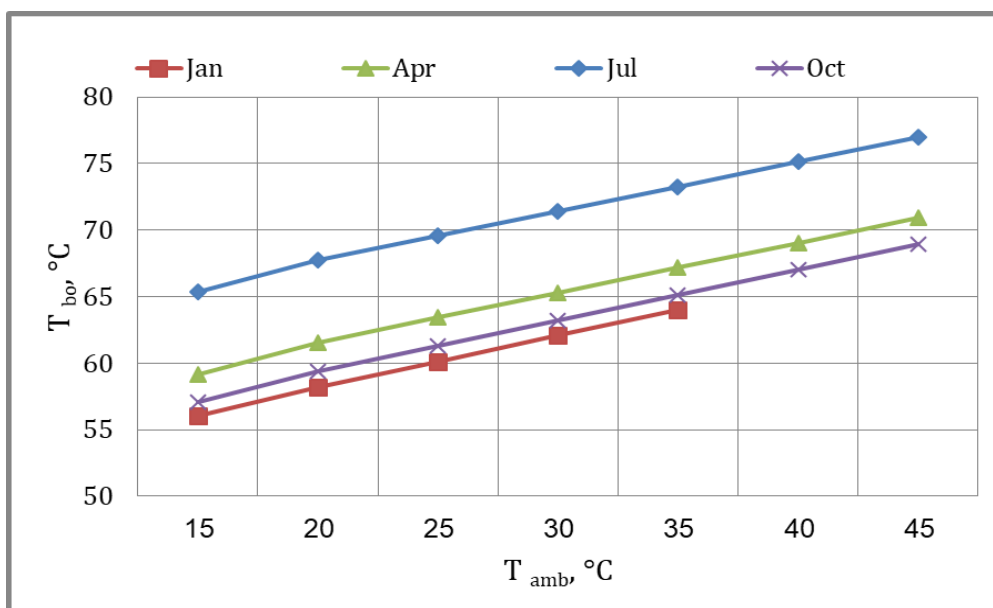

Fig. 13 Effect of ambient temperature on the bed outlet adsorbate temperature for different seasons

It was also found that the highest bed outlet adsorbate temperature was in July, April, October, and January. As a result of the collector water in the bed, heat exchange occurred between the adsorbate and the collector water, which led to an increase in the bed outlet adsorbate temperature and a decrease in the temperature of the collector water.

Figure 14 shows the effect of ambient temperature on the condenser output adsorbate temperature for different seasons. The figure indicates that the condenser output adsorbate temperature increased when the ambient temperature increased. In April, the condenser outlet adsorbate temperature increased from 49.18 °C to 60.94 °C, an increase of 23.9 %, when the ambient temperature changed from 15 °C to 45 °C, an increase of 200 %. It was also found that the highest condenser outlet adsorbate temperature was in July, April, October, and January. An increase in the ambient temperature, the bed outlet temperature, and the collector's water temperature outlet lead to an increase in the adsorbate temperature at the outlet of the condenser.
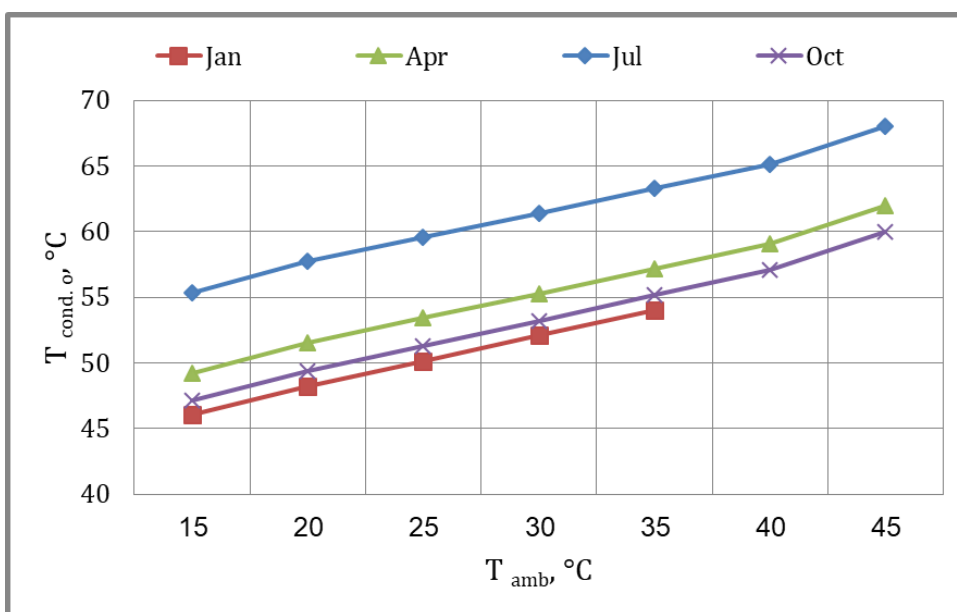

Fig. 14 Effect of ambient temperature on the condenser outlet adsorbate temperature for different seasons.

Figure 15 shows the ambient temperature's effect on the evaporator thermal power for different seasons The figure indicates that the evaporator thermal power increased when the ambient temperature increased. In April, the evaporator thermal power increased from 5.78 kW to 6.85 kW, with an increase of 18.5 %, when the ambient temperature changed from 15 °C to 45 °C with an increase of 200 %.
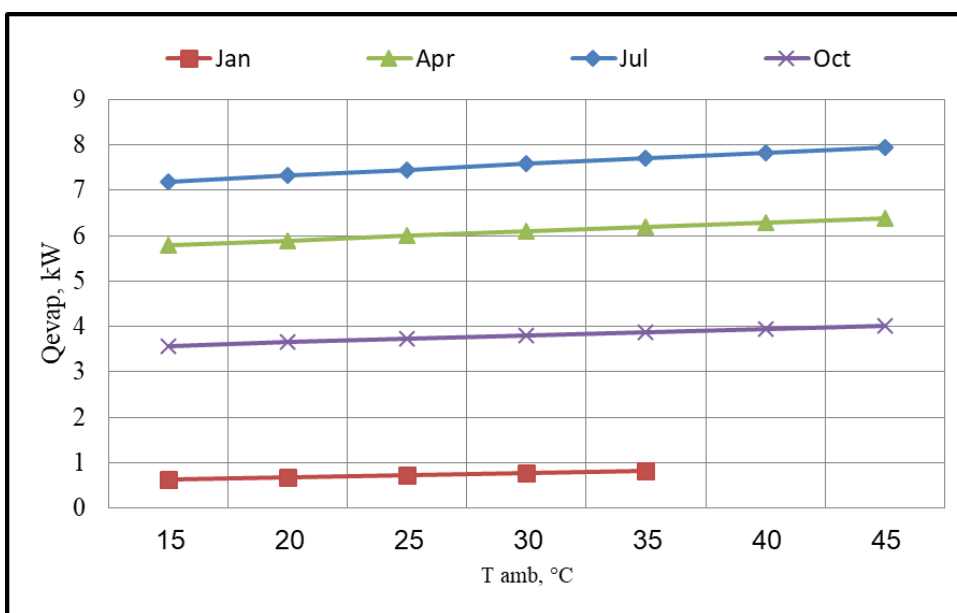

Fig. 15 Effect of ambient temperature on the evaporator thermal power for different seasons.

It was also found that the highest evaporator thermal power was in July, April, October, and January. The results showed that increasing the ambient temperature increased the condenser output adsorbate temperature. Thus, the output condenser enthalpy increased, which increased the evaporator's thermal power.

Figure 16 shows the ambient temperature's effect on SCP for different seasons. The figure indicates that SCP increased when the ambient temperature increased. In April, SCP increased from 251.5 W/kg to 277.6 W/kg, with an increase of 10.4 %, when the ambient temperature changed from 15 °C to 45 °C with an increase of 200%. It was also found that the highest SCP was in July, April, October, and January. Increasing the SCP depends on increasing the evaporator thermal power, which is at a constant amount of silica gel.
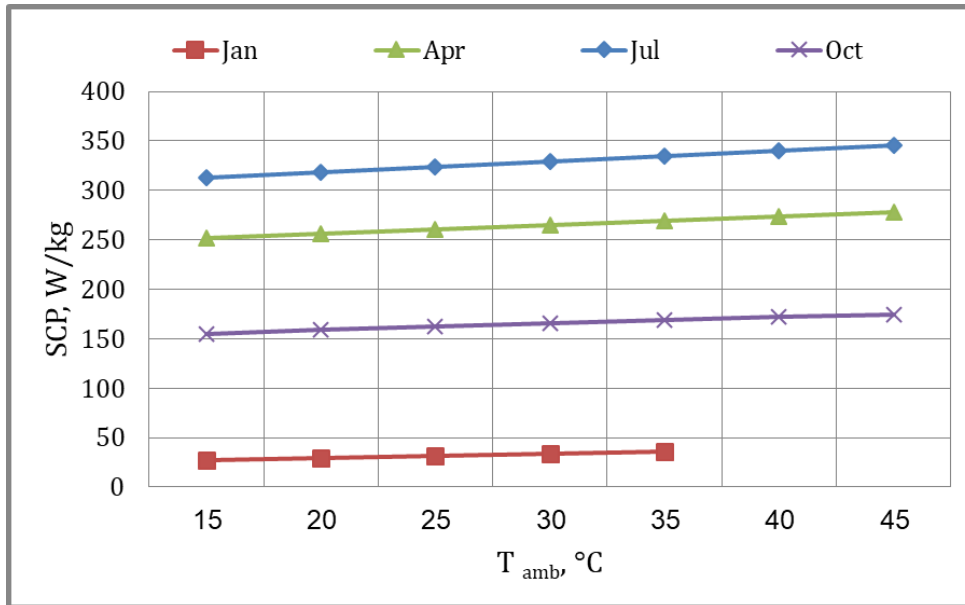

Fig. 16 Effect of ambient temperature on SCP for different seasons.

Figure 17 shows the ambient temperature's effect on COP for different seasons. The figure indicates that COP increased when the ambient temperature increased. In April, COP increased from 0.6 to 0.63, with an increase of 5 %, when the ambient temperature changed from 15 °C to 45 °C with an increase of 200 %.
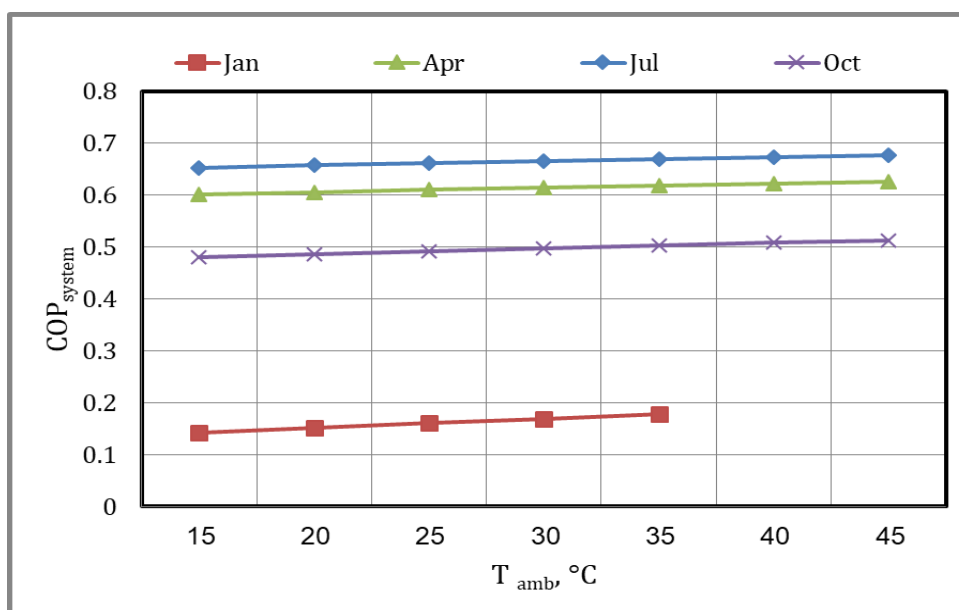

Fig. 17 Effect of ambient temperature on COP for different seasons

. It was also found that the highest COP was in July, April, October, and January. The results showed that the COP at the ambient temperature of 30 °C in January was 0.17, in October was 0.5, in April was 0.61, and in July was 0.67; this explains that the COP increased with the increase in solar radiation.

Figure 18 shows the ambient temperature's effect on the COP solar system. It shows that COP solar system increased when the ambient temperature increased. In April, when the ambient temperature changed from 15 °C to 45 °C with an increase of 200 %, the COP solar system increased from 0.382 to 0.422, with an increase of 10.5 %. It was also found that the highest COP solar system was in July, April, October, and January. Results indicated that the COP solar system at the ambient temperature of 30 °C in January was 0.114, in October was 0.332, in April was 0.403, and in July was 0.425; this explains that the COP increased with the increase in solar radiation.
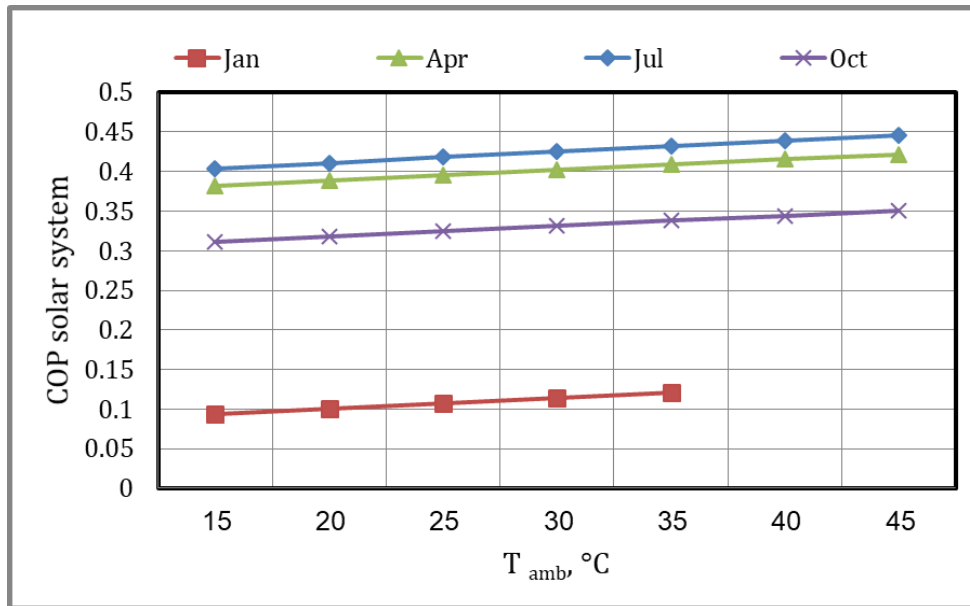

Fig. 18 Effect of ambient temperature on COP solar system for different seasons

5.2 Effect of the collector water outlet temperature:

Figure 19 shows the collector water outlet temperature's effect on COP for different seasons. The figure indicates that COP decreased when the collector water outlet temperatures increased.
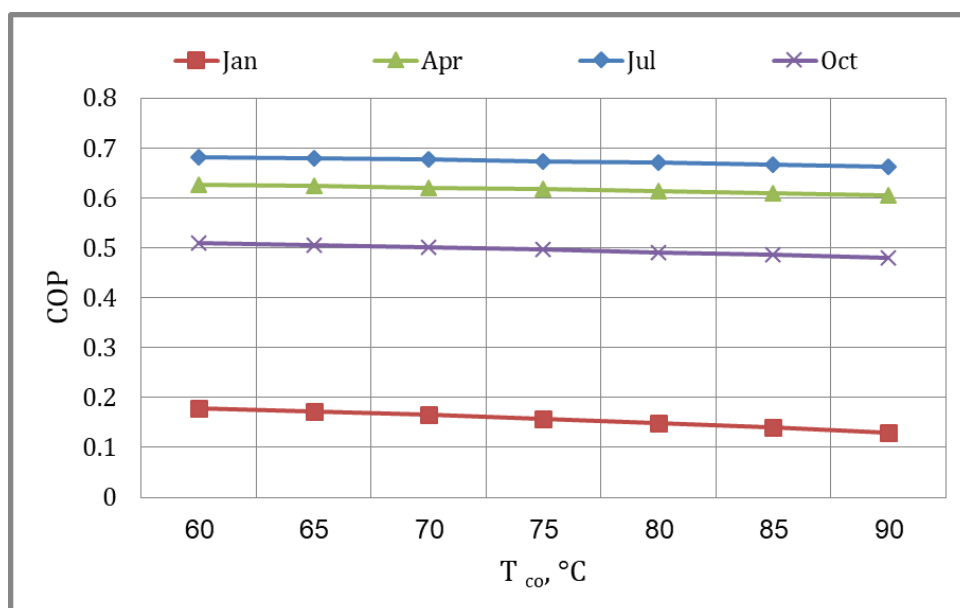

Fig. 19 Effect of the collector water outlet temperature on COP for different seasons

In April, when the collector water outlet temperature changed from 60 °C to 90 °C with an increase of 50 %, COP decreased from 0.627 to 0.604, with a decrease of 3.7 %. It was also found that the highest COP was in July, April, October, and January. The results showed that the COP at the collector water outlet temperature of 75 °C in January was 0.158, in October was 0.496, in April was 0.617, and in July was 0.674.

Figure 20 shows the collector water outlet temperature's effect on SCP for different seasons. The figure indicates that SCP decreased when the collector water outlet temperature increased. In April, SCP decreased from 284.11 to 250.19 W/kg, with a decrease of 12 %, when the collector water outlet temperature changed from 60 °C to 90 °C with an increase of 5 0%. It was also found that the highest SCP was in July, April, October, and January. The results showed that the SCP at the collector water outlet temperature of 75 °C in January was 31 W/kg, in October was 163 W/kg, in April was 268 W/kg, and in July was 345 W/kg.
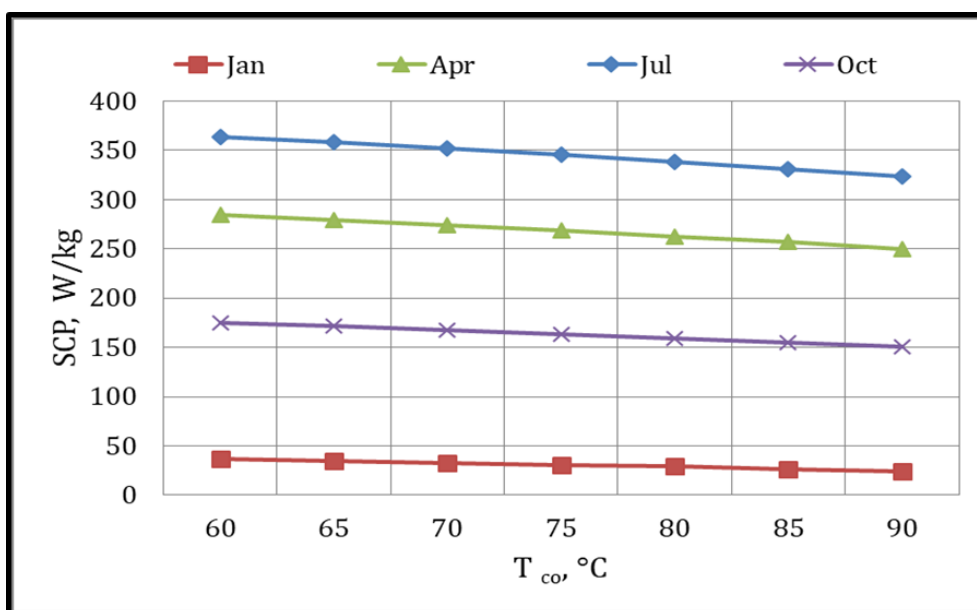

Fig. 20 Effect of the collector water outlet temperature on SCP for different seasons

5.3 Effect of the collector area:

The effect of the collector area on COP for different seasons is presented in Figure 21. It shows that the COP system increased when the collector area increased
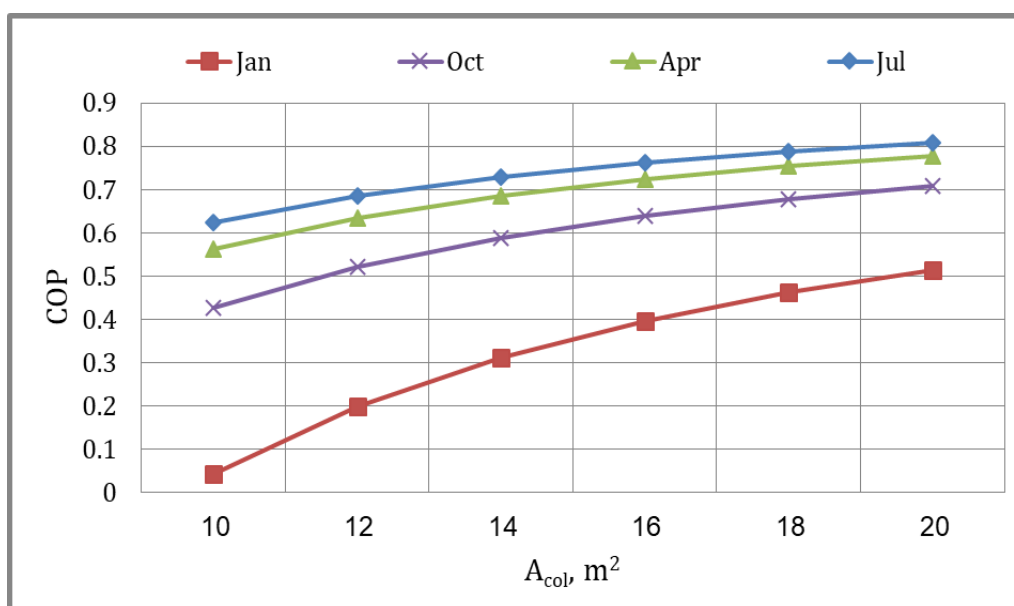

Fig. 21 Effect of the area of the collector on COP for different seasons

In April, the system COP increased by 0.562: 0.777, with an increase of 38.25 % when the collector area changed from 10 m2 to 20 m2. It was also found that the highest COP system was found in July, April, October, and January, respectively. The results showed that the COP system at the collector area of 16 m2 in January was 0.397, in October was 0.639, in April was 0.723, and in July was 0.762; this explains that the COP increased with the increase in solar radiation.

While the effect of the area of the collector on SCP for different seasons is shown in Fig. 22. It is found that the SCP increased when the collector area increased. In April, when the collector area changed from 10 m2 to 20 m2, SCP increased from 194.5 W/kg to 524.1 W/kg, with an increase of 169.5 %. It was also found that the highest SCP was found in July, April, October, and January, respectively. The results showed that the SCP at the collector area of 16 m2 in January was 100.3 W/kg, in October was 268.3 W/kg, in April was 394.6 W/kg, and in July was 478.3 W/kg; this explains that the SCP is greatly affected by solar radiation.
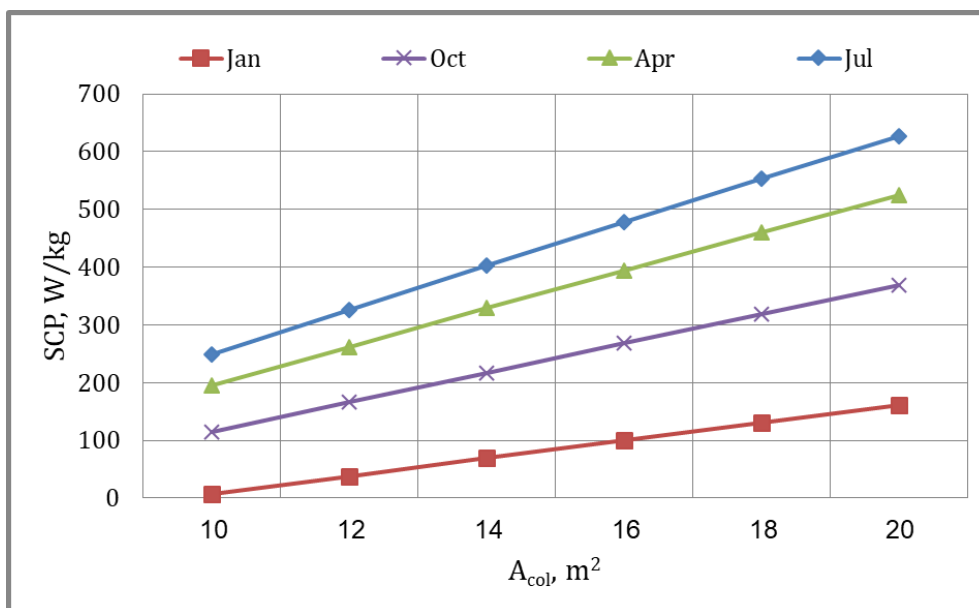

Fig. 22 Effect of the collector area on SCP for different seasons

The effect of the collector area on the cooling capacity for different seasons is shown in Fig. 23.
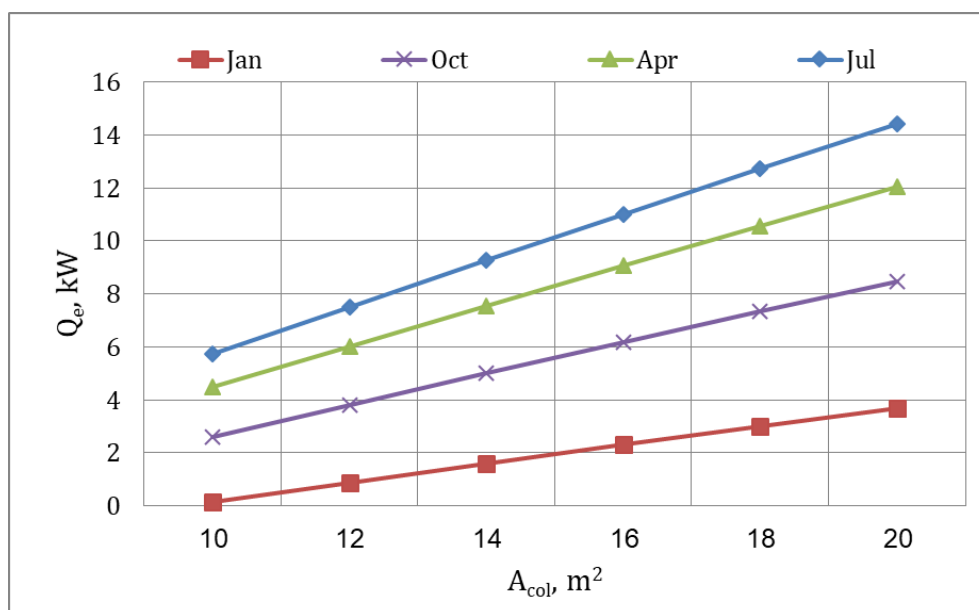

Fig. 23 Effect of collector area on the cooling capacity for different seasons

The system cooling capacity is achieved in winter with a collector area of 20 m2 and in autumn with a collector area of 12 m2, while it is achieved in Summer and Spring with a collector area of less than 10 m2.

6. Validation

To provide validation of the present study, a comparison of the output results of one of the published works of literature [El-Sharkawy et al. 2014]. and present work for the conditions is shown in Fig. 24. The comparison was made to estimate the COP as a function of collector output temperature on the same operating conditions; cooling capacity 4.2 TR, ambient temperature 35 oC, Condenser temperature 40 oC, and Evaporator temperature 10 oC.   It is found that there is considerable agreement between the current study and the previously published work under the same operating conditions. The slight deviation between the results is due to some assumptions in the current simulation study.
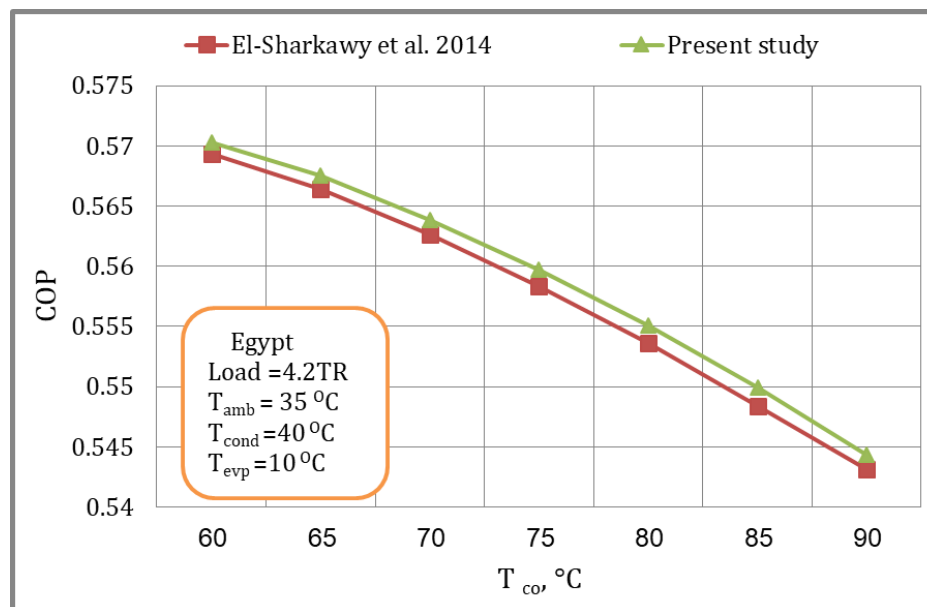

Fig. 24 compares the current study's collector water outlet temperature and the literature [El-Sharkawy et al. 2014].

7. Conclusions

This work was performed using Matlab software to evaluate the performance of a   3.5kW solar silica gel/water adsorption cooling system. They studied the effect of the atmospheric air temperature on the collector water outlet temperature, the collector efficiency, the collector thermal power, the bed thermal power, the collector water inlet temperature, the bed outlet adsorbate temperature, the condenser output adsorbate temperature, the evaporator thermal power, SCP and COP at different seasons of the year. The following remarks can be concluded:

- The collector thermal power, evaporator thermal power, and bed thermal power increased with the ambient temperature increase at different seasons of the year.
- The collector water outlet temperature, the collector efficiency, the collector water inlet temperature, the bed outlet adsorbate temperature, and the condenser outlet adsorbate temperature increased with the ambient temperature increase at different seasons of the year.
- SCP and COP increased with increased ambient temperature and the collector area at different seasons. At the same time, SCP and COP decreased with the increase of the collector water outlet temperature at different seasons.
- The highest COP and SCP at the ambient temperature of 30°C were 0.68 and 345 W/kg, the collector output temperature of 75 °C was 0.67 and 355 W/kg, and the collector area of 14 m2 was 0.81 and 626 W/kg, respectively.
- The system cooling capacity is achieved in winter with a collector area of 20 m2 and in autumn with a collector area of 12 m2, while it is achieved in Summer and Spring with a collector area of less than 10 m2.
- It is recommended to study the effect of the mass flow rate of the collector, chilled water, and adsorbate and the effect of the temperature of the evaporator and condenser on the system performance.

8. Nomenclature

Cp	Heat Capacity at constant pressure, kJ/kg. °C
Ex	Exergy, kW
h	Enthalpy, kJ/kg
I	irreversibility rate, kW
IS	Solar Radiation, W/m2
M	Mass Flow Rate, kg/s
OH	Operation Hours, h.
P	Pressure, Bar
PR	Pressure Ratio
Q	Thermal power, kW
S	Entropy, kJ/kg.K
T	Temperature, °C
V	Velocity, m/s
U	Overall energy loss, kW/m2. °C
W	Equipment power, kW
X	Water uptake of silica gel

Subscripts

amb	Ambient
b	Bed
c	collector
chw	Chilled water
col	Collector
cond	Condenser
evap	Evaporator
i	Inlet
o	Outlet
p	pump
r	Refrigerant
SG	Silica gel
t	Tube
w	Water
η	
Δ	
ρ	

9. References

[1]   C.J. Chen, R.Z. Wang, Z.Z. Xia, J.K. Kiplagat, "Study on a silica gel–water adsorption chiller integrated with a closed wet cooling tower", International Journal of Thermal Sciences, Vol. 49, PP. 611-620, 2010.

[2]   C.J. Chen, R.Z. Wang, Z.Z. Xia, J.K. Kiplagat, Z.S. Lu, "Study on a compact silica gel–water adsorption chiller without vacuum valves: Design and experimental study", Applied Energy, Vol. 87, PP. 2673-2681, 2010.

[3]   Rezk, R. Al-Dadah, S. Mahmoud, A. Elsayed, "Characterisation of metal-organic frameworks for adsorption cooling", International Journal of Heat and Mass Transfer, Vol. 55, PP 7366-7374, 2012.

[4]   Rezk, and R. K. Al-Dadah, "Physical and operating conditions effects on silica gel-water adsorption chiller performance", Applied Energy, Vol. 89, Pp. 142-149, 2012.

[5]   A Rezk, R Al-Dadah, S Mahmoud and A Elsayed," Experimental investigation of metal-organic frameworks characteristics for water adsorption chillers", J Mechanical Engineering Science, Vol.227, No. 5, Pp. 992-1005, 2012.

[6]   Rezk, R. AL-Dadah, S. Mahmoud, B. Shi and A. Elsayed," Ethanol adsorption characteristics on metal-organic frameworks for cooling applications", International Conference on Applied Energy, 10630, 2012.

[7]   Rezk, R.K. Al-Dadah, S. Mahmoud, A. Elsayed, "Effects of contact resistance and metal additives in finned-tube adsorbent beds on the performance of silica gel/water adsorption chiller", Applied Thermal Engineering, Vol. 53, PP 278-284, 2013.

[8]   D. Wang, J. Zhang, Q. Yang, N. Li, K. Sumathy," Study of adsorption characteristics in silica gel–water adsorption refrigeration", Applied Energy, Vol. 113, PP 734–741, 2014.

[9]   I. El-Sharkawy, H. Abdel Meguid, B. B. Saha, "Potential application of solar powered adsorption cooling systems in the Middle East", Applied Energy, Vol. 126, Pp. 235-245, 2014.

[10] P. G. Youssef, R. AL-Dadaha, S. Mahmoud, H. Dakkamaa, A. Elsayed, "Effect of the evaporator and condenser temperature on the performance of Adsorption desalination Cooling cycle", Energy Procedia, Vol. 75, PP. 1464-1469, 2015.

[11] Khalil, S. A. El-Agouz, Y. A. F. El-Samadony, and M. A. Sharaf, " Experimental study of silica gel/water adsorption cooling system using a modified adsorption bed", Science and Technology for the Built Environment, Vol. 22, PP 41–49, 2016.

[12] D. D. Kumar, S. A. M. Krishna, S. Kasthurirengan, G. B. Krishnappa," An experimental investigation on adsorption refrigeration system using silica gel-water", Journal of Mechanical Engineering and Biomechanics, Vol. 1, No. 1, PP 56-63, 2016.

[13] G. Najeh, G. Slimane, M. Souad, B.r Riad, G. Mohammed, "Performance of silica gel-water solar adsorption cooling system", Case Studies in Thermal Engineering, Vol. 8, PP. 337-345, 2016.

[14] Ghilen N, Gabsi S, Benelmir R, Ganaoui ME, "Performance Simulation of Two-Bed Adsorption Refrigeration Chiller with Mass Recovery" J. Fundam Renewable Energy Appl., Vol. 7, No. 3, PP. 1-7, 2017.

[15] Ghilen Najeh, Messai Souad, Gabsi Slimane, El Ganaoui Mohammed, and Benelmir Riad, "Numerical Investigation of Silica Gel-Water Solar Adsorption Cooling System with Simulink", American Journal of Applied Sciences, Vol. 14, No. 8, PP. 786-794, 2017.

[16] Najeh Ghilen, Souad Messai, Slimane Gabsi, Mohammed El Ganaoui, and Riad Benelmir, "Performance Simulation of Two-Bed Silica Gel-Water Adsorption Chillers", Global Journal of Researches in Engineering, Vol. 17, No. 3, PP. 41-49, 2017.

[17] Szelągowski and A. Grzebielec, "Performance comparison of a silica gel-water and activated carbon-methanol two beds adsorption chillers", E3S Web Conf., Vol. 17, PP 1-8, 2017.

[18] K. Lim, J. Che, and J. Lee," Experimental study on adsorption characteristics of a water and silica-gel based thermal energy storage (TES) system" Applied Thermal Engineering, Vol. 110, PP 80–88, 2017.

[19] S. Mitra, K. Thu, B. B. Saha, P. Dutta, "Modeling the effect of heat source temperature on the performance of two/stage air cooled silica gel-water adsorption system" Energy Procedia, Vol. 105, PP. 2010-2015, 2017.

[20] S. Mitra, K. Thu, B. B. Saha, P. Dutta, "Performance evaluation and determination of minimum desorption temperature of a two-stage air-cooled silica gel/water adsorption system" Applied Energy, Vol. 206, PP 507-518, 2017.

[21] M. L. Ntsoane, A. Jalali, J. Römer, K. Duewel, C. Göller, R. Kühn, K. Mähne, M. Geyer, D. Sivakumar, and P. V. Mahajan, "Performance evaluation of silica gel-water adsorption based cooling system for mango fruit storage in Sub-Saharan Africa" Postharvest Biology and Technology, Vol. 149, PP. 195-199, 2019.

[22] M. M. Abd-Elhady and A. M. Hamed, "Effect of fin design parameters on the performance of a two-bed adsorption chiller", International Journal of Refrigeration, Vol. 113, PP 164–173, 2020.

[23] M. Kilic and M. Anjrini, "Comparative performance evaluation of the mechanical and adsorption hybrid cooling systems for the cascaded and the serial connected evaporator's configurations," Case Studies in Thermal Engineering, Vol. 28, PP. 101489, 2021.

[24] M. B. Elsheniti, A. T. Abd El-Hamid, O. A. El- Samni, S. M. Elsherbiny, E. Elsayed "Experimental evaluation of a solar two-bed lab-scale adsorption cooling system" Alexandria Engineering Journal, Vol. 60, PP. 2747–2757, 2021.

[25] Mostafa, M. Hassanain, E. Elgendy, "Transient simulation and design parameters optimization of a cold store utilize solar assisted adsorption refrigeration system," Case Studies in Thermal Engineering, Vol. 37, 102273, 2022.

[26] K. Missaoui, A. Kheiri, N. Frikha, S. Gabsi, M. El Ganaou, "Heat storage in solar adsorption refrigeration systems: A case study for indigenous fruits preservation", Case Studies in Thermal Engineering, Vol. 40, 102472, 2022.

[27] Z. Wang, Z.Yuan, C. Du, Y. Liu, J. Wang, "Performance of solar adsorption cooling system with internal finned vacuum tube bed", Case Studies in Thermal Engineering, Vol. 34102063, 2022.

[28] H.H. El-Ghetany, M. A. Omara, R. G. Abdel hady, Gamal. B. Abdelaziz, "Design of Silica Gel/Water Adsorption Chiller Powered by Solar Energy for Air Conditioning Applications", Journal of Energy Storage, Vol. 63, 107055, July 2023.